efficiency decreases there is a fast component to the decay which increases in strength whilst, at long times, the same slow decay is observed. This is the form of the data predicted by the tunnelling model, and there is qualitative agreement with the model, although the distributed radiative decay times makes it difficult to calculate the exact form of the decay (Tsang and Street 1978, 1979, Austin *et al.* 1979 a). These results are therefore a further demonstration of the tunnelling model. We also note that there is at least one analogous situation in a crystal. In GaP containing nitrogen, radiation recombination of a bound exciton competes with phonon assisted tunnelling to random localized states (Wiesner *et al.* 1975). The same changes in luminescence quantum efficiency and two component decay is observed.

The tunnelling model can be extended to higher temperatures. Above 50 K ionization of the election–hole pair introduces a different temperature dependent non-radiative mechanism (see § 2.3.3). This mechanism reduces the time available for tunnelling to the defect and therefore we expect tunnelling to become relatively less important as the temperature increases. Figure 12 shows the temperature dependence of luminescence for samples of different defect density. It can be seen that, although the low temperature luminescence efficiency varies because of the different defect densities, at high temperatures the curves converge in accordance with our expectations. Thus there is a progressive transfer from one non-radiative mechanism to the other.

2.3.3. *Temperature dependence*

So far we have mostly dealt with the low temperature limit in which the assumption of carriers frozen into localized states after thermalization is adequate. At high temperatures thermally activated diffusion of carriers is expected to affect the recombination mechanisms. Apart from the obvious change in the luminescence intensity shown in fig. 12, thermal effects are observed in the luminescence decay as

Fig. 12

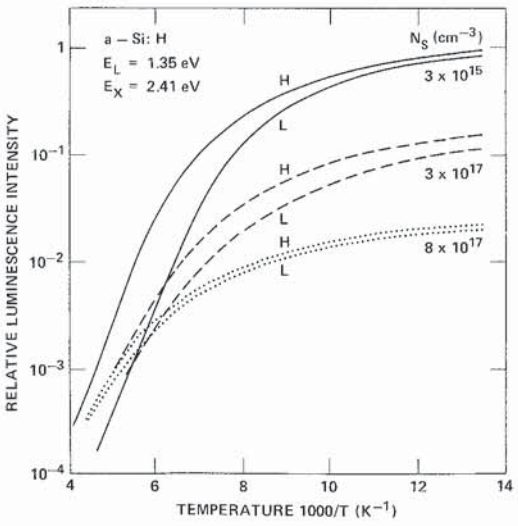

Temperature dependence of the luminescence intensity for samples of different defect density observed at high (H) and low (L) excitation intensities. Note the convergence of the data at high temperature. The intensity dependence is described in § 2.3.3 (Street 1981 a).

shown in fig. 10. The data can be divided into two regions. Below 50 K the luminescence efficiency y_L is approximately constant or increases with temperature (see § 2.3.4), but the mean lifetime τ decreases. Above 50 K there is a much larger change and both y_L and τ decrease rapidly. The luminescence intensity and the lifetimes are related to the competing rates for radiative, P_R, and non-radiative, P_{NR}, recombination by the expression

$$y_L = P_R/(P_R + P_{NR}) = P_R\tau, \tag{19}$$

$$\tau = (P_R + P_{NR})^{-1}. \tag{20}$$

It is then easy to see that if y_L increases but τ decreases then P_R must be increasing, and so it is concluded that in the low temperature region the radiative rate increases slowly. Above 50 K the parallel decreases in y_L and τ shows that non-radiative processes are dominating.

These results are interpreted with the models of geminate recombination used to account for the properties at low temperature, and more generally applied to amorphous semiconductors (Onsager 1938, Davis 1970, Pai and Enck 1975). Figure 13 illustrates that after thermalization the electron and hole have separated, but remain bound by their mutual Coulomb interaction. As the temperature is increased the electron diffuses and will first tend to move towards the hole under the Coulomb attraction. This motion will reduce the radiative decay time because the overlap increases. At higher temperatures, however, the electron has enough thermal energy to escape from the hole and radiative recombination does not occur. In this model, the rate limiting process in the non-radiative process is the escape of the electron, even though this is not an actual non-radiative process. The ultimate fate of the free electron is discussed in more detail in § 2.3.4.

This model is supported by calculations of the rate of diffusion of the carrier (Noolandi *et al.* 1980 a, b, Hong *et al.* 1981). The calculation solves the time dependent diffusion equation for the distribution of the carrier and assumes that the

Fig. 13

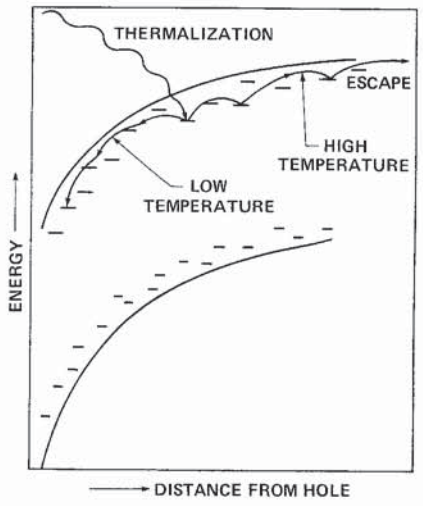

Schematic diagram of the Onsager model of thermalization and geminate recombination as applied to a-Si : H.

Fig. 14

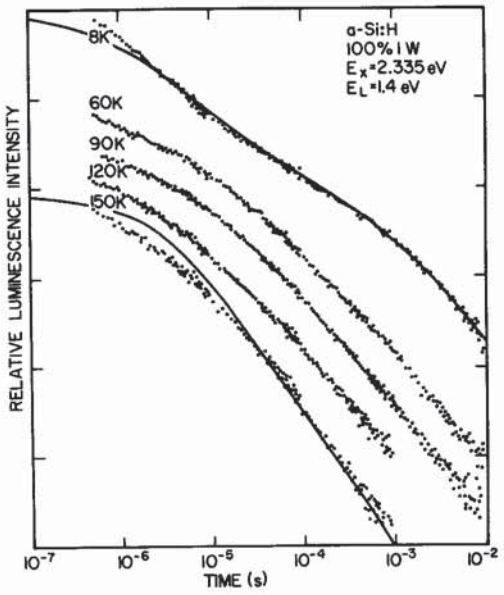

Temperature dependence of the luminescence decay. Solid curves are the fit to theory (Noolandi *et al.* 1980 b).

radiative process is tunnelling as given by eqn. (12). The initial distribution of pair separations immediately after thermalization is found from the luminescence decay as described in §2.3.1. A particular diffusion coefficient is assumed and the time dependence of the decay is calculated. Figure 14 shows that this calculation gives a good fit to the data. In particular there is an asymptotic solution for the decay of the luminescence intensity

$$I(t) \sim t^{-3/2}, \tag{21}$$

which is observed in the data. Figure 14 shows that the high temperature data is qualititatively different from the low temperature decay for which diffusion is believed to be negligible. The calculation also results in values of the diffusion coefficient which are consistent with the known electron mobility.

There have been many reports of the temperature dependence of the luminescence intensity (Engemann and Fischer 1973, Tsang and Street 1979, Austin *et al.* 1979 a, Collins *et al.* 1980 b). All find qualitatively similar data, although widely different values of the activation energy. In fact, there is not a single activation energy and as shown in fig. 15, in many cases there is a better fit to an expression of the form (Collins *et al.* 1980 b)

$$(1/y_L - 1)^{-1} = y_0 \exp(-T/T_0). \tag{22}$$

It is known that photoluminescence in chalcogenide glasses tends to follow this expression (Street *et al.* 1974) although its physical significance is not clear and several suggestions for the origin have been suggested. We take this opportunity to promote a likely candidate suggested by Higashi and Kastner (1979). It is assumed

Fig. 15

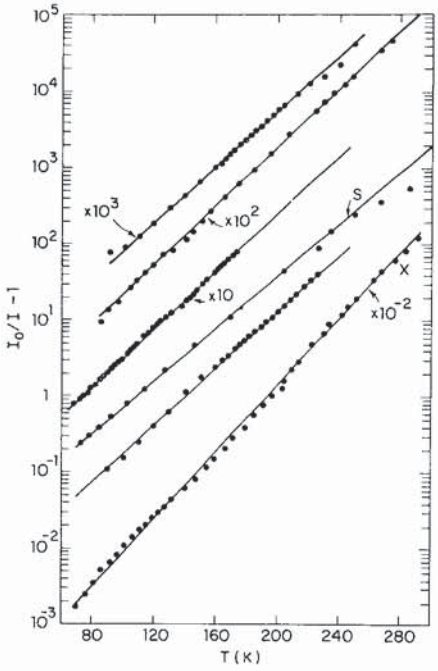

Temperature dependence of the luminescence intensity plotted to show the fit to eqn. (22). Curve S is replotted from Austin *et al.* (1979 a) and curve X from Tsang and Street (1979) (Collins *et al.* 1980 b).

that there is an exponential distribution of band tail states $\exp(-w/w_0)$ where w is measured from the mobility edge. Next a binding energy E_D is defined such that

$$\tau_R^{-1} = \nu_0 \exp(-E_D/kT), \tag{23}$$

where ν_0 is the usual prefactor $\sim 10^{12}\,s^{-1}$. E_D is therefore the energy for which the release to the mobility edge has the same probability as radiative recombination. All shallower states will tend to be released and diffuse away whereas deeper states recombine radiatively. Assuming a random population of tail states, the quantum efficiency will be given approximately by

$$y_L = \int_{E_D}^{\infty} \exp(-w/w_0)\,dw \Big/ \int_0^{\infty} \exp(-w/w_0)\,dw$$
$$= \exp(-E_D/w_0). \tag{24}$$

Substituting for E_D from eqn. (23) gives

$$y_L = \exp(-kT \ln(\nu_0\tau_R)/w_0), \tag{25}$$

which is of the form of eqn. (22) (for $y_L \ll 1$) with

$$T_0 = w_0/k \ln(\nu_0\tau_R) \simeq w_0/20\,k, \tag{26}$$

assuming $\tau_R \sim 10^{-3}$ s. The observed data have $T_0 \sim 23$ K (Collins *et al.* 1980 b) which gives $w_0 \sim 0{\cdot}04$ eV which seems a plausible value for a band tail.

Some interesting data which support this model is the observed temperature shift of the luminescence peak position. Data for glow discharge samples are shown in fig. 16 and above 100 K the peak energy has a temperature coefficient of $1{\cdot}8 \times 10^{-3}$ eV/K compared to a coefficient of $4{\cdot}3 \times 10^{-4}$ eV/K for the band gap (Tsang and Street 1979). Austin *et al.* (1979 a) report a coefficient of $1{\cdot}6 \times 10^{-3}$ eV/K, which is in good agreement. The much larger shift of the peak can be explained by the ionization of the shallow bound carriers, leaving recombination between deeper states and resulting in a lower energy of the luminescence. If we use the position of E_D as a marker of the shift of the luminescence peak, then a temperature coefficient of $20k$ or $1{\cdot}7 \times 10^{-3}$ is predicted, which is in fairly good agreement with the amount by which the observed shift exceeds that of the band gap energy. In sputtered samples, the shift of the peak is much smaller ($2{\cdot}3 \times 10^{-4}$ eV/K) and approximately follows the band gap (Paesler and Paul 1980). The reason for the different behaviour is unclear. It is also worth noting that the luminescence peak in chalcogenide glasses shifts to a higher rather than lower energy (Kolomiets *et al.* 1972), suggesting that a different mechanism operates in this case.

The thermally activated release of carriers from an exponential band tail has also been used to explain the dispersive transport properties of both a-Si : H (Tiedje and Rose 1981) and chalcogenides (Orenstein and Kastner 1981). According to this model, the dispersion parameter α is given by T/T_L, where T_L is w_0/k. Thus

$$T_L = 20T_0 = 460\ \text{K}. \tag{27}$$

In samples which give the above luminescence data, $T_c \sim 600$ K from transient photoconductivity data (Street 1981). However, other reports (Tiedje *et al.* 1981) give smaller values of T_L, and it would be interesting to measure the luminescence of such samples.

It should be recognized that the assumptions of this model contrast with those used to describe the temperature dependence of the decay. In one case the energy distribution is ignored and the recombination rate is assumed to be governed by diffusion. In the other case the energy distribution is considered and diffusion is not. Instead the electron is assumed either to be localized or to have escaped. Clearly the

Fig. 16

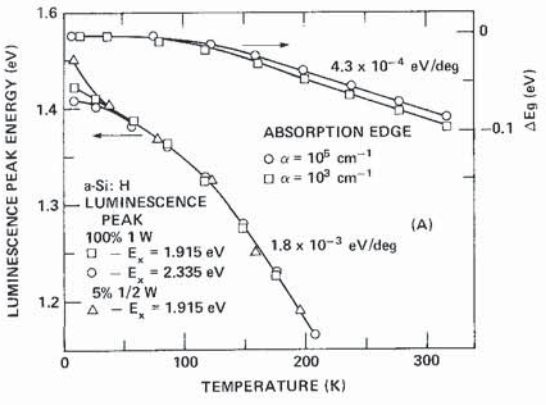

Temperature dependence of the luminescence peak energy compared to the much smaller shift of the gap (Tsang and Street 1979).

reality lies in between. One must consider both the distribution of states and the diffusion of carriers. It is not obvious how good a description of the process is given by either model. The combined effects may be difficult to calculate, but may be susceptible to a computer simulation.

2.3.4. *High excitation intensities*

The decay data discussed in §2.3.1 referred to low excitation intensities. In this section we describe some effects of a moderately strong illumination and their interpretation. Figure 17 shows data in which it is found that the decay times tend to decrease as the excitation intensity increases (Tsang and Street 1979). Figure 18 shows there is a value of the excitation intensity below which the decay is constant and above which it decreases. This represents a transition from monomolecular to bimolecular recombination kinetics. The model to explain this behaviour is again based on the ideas of geminate recombination (Onsager 1938) which were discussed in §2.3.3. A characteristic feature of amorphous materials is a very short carrier mean free path which allows rapid thermalization to the band tail states. It is widely believed that after optical excitation of an electron–hole pair, the carriers will diffuse apart a distance R which is only some tens of ångströms before being trapped in the band tails. When this occurs at low temperatures, further diffusion ceases. We now assume that the excitation intensity G is such that the electron-hole pair density is N. ($N=G\tau$, where τ is the average lifetime). The mean separation D of pairs is given roughly by

$$D=N^{-1/3}. \tag{28}$$

If G is chosen such that D is much larger than R then it is clear that the pairs will be isolated and must recombine geminately in a monomolecular process. On the other hand, if D is less than R the electron–hole pairs overlap substantially and their

Fig. 17

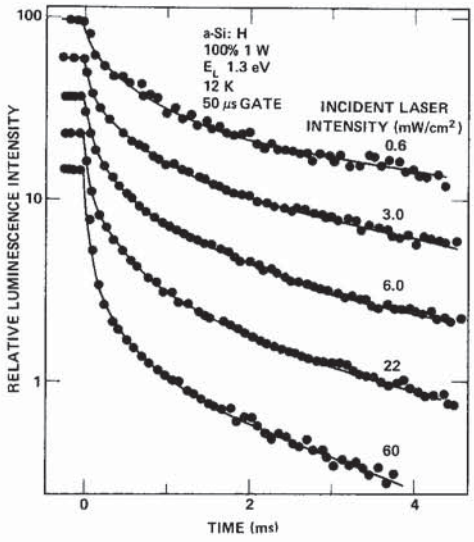

Examples of the luminescence decay at difference excitation intensities (Tsang and Street 1979).

Fig. 18

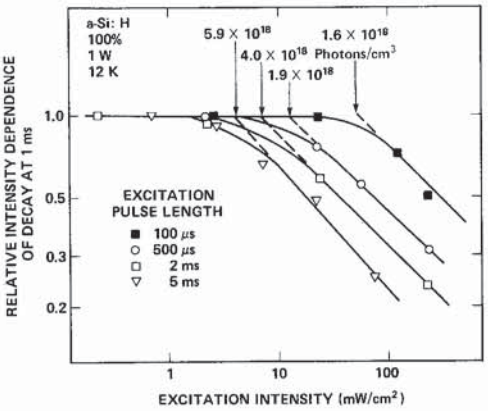

Dependence of the luminescence decay on excitation energy for different excitation pulse lengths. The change of slope marks the transition from monomolecular to bimolecular decay (Tsang and Street 1979).

geminate identity is lost. In this case a bimolecular recombination mechanism appropriate for a randomly dispersed sea of electron and holes is expected. These two regions of recombination kinetics are seen in fig. 18. According to the above argument, the transition occurs when $R = D$ and so it is of interest to determine N at the transition point. This has been done for all the different pulse lengths shown in fig. 18, and when a correction is made for the known distribution of decay times, a common value of $1{\cdot}5 \times 10^{18}$ cm^{-3} is obtained, which corresponds to a value for D of ~ 50 Å. This compares favourably with the mean value of the separation R obtained from the low intensity distribution of decay times (Tsang and Street 1979), and from the value of the Bohr radius obtained from the dependence of the luminescence intensity on the defect density (Street *et al.* 1978 b).

High excitation intensities also affect the luminescence temperature dependence. Figure 19 shows data in which the low temperature increase of intensity disappears at sufficiently low excitation intensity (Street 1981). From this data a new non-radiative process which is most effective at low temperature and high excitation intensity is deduced. The intensity at which the mechanism occurs corresponds roughly to the onset of the bimolecular process. Figure 20 shows the intensity dependence of luminescence which becomes sublinear when the photo-excited pair density exceeds 10^{18} cm^{-3}, again indicating a non-radiative process at high intensity (Shah *et al.* 1980 b). Similar data are reported by Paesler and Paul (1980), and Rehm and Fischer (1979).

It is argued that these results are due to an Auger mechanism (Street 1981 a, Rehm and Fischer 1979). The Auger process cannot occur for isolated geminate pairs since at least three carriers are needed. Thus the mechanism is expected to become important when the intensity for the bimolecular process is reached and pairs overlap, in agreement with the observations. There are no calculations of the Auger rate for the present experimental situation, but it seems likely that the rate is adequate to give the observed effects.

The identification of the Auger mechanism necessitates a re-evaluation of the data in fig. 18. It is not immediately clear to what extent the decreasing lifetime is

Fig. 19

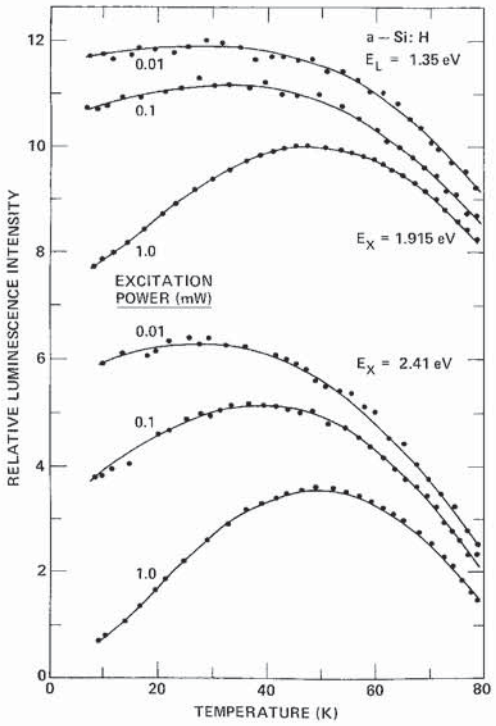

Temperature dependence of the luminescence intensity for different excitation intensities (Street 1981 a).

Fig. 20

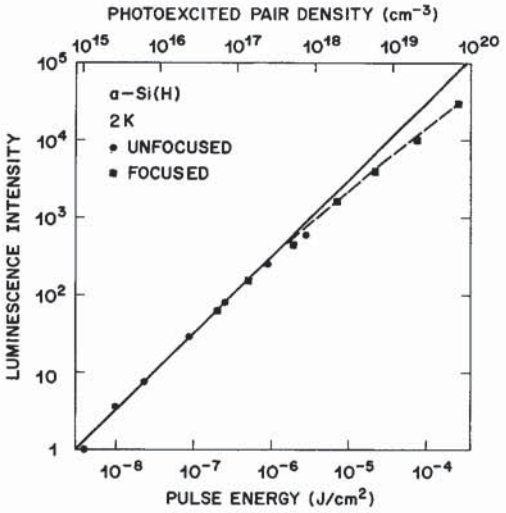

Intensity dependence of the luminescence intensity showing the sublinear behaviour where the pair density exceeds about $10^{18}\,cm^{-3}$ (Shah *et al.* 1980 b).

due to the bimolecular radiative process or the non-radiative Auger process. The indication from both figs. 19 and 20 is that the Auger process is a relatively weak mechanism because the luminescence efficiency doesn't drop by more than a factor of 2. The bimolecular radiative rate is governed by the separation of a neighbouring electron and hole whilst the Auger rate depends on the separation of two electrons or holes. Thus the dominant process is likely to be determined by the local configuration at any site.

At temperatures above 50 K there are different intensity dependent effects, which increase the luminescence efficiency as indicated in fig. 12. Figure 21 shows data at 170 K for samples of varying defect density (Street 1981 a). The quantum efficiency is seen to increase most in the samples of the lowest defect density. The explanation of this effect given by Street (1981 a) is as follows. As described in § 2.3.3, the primary rate-limiting process in the non-radiative mechanism at high temperatures is the thermally activated diffusion apart of electron–hole pairs. It is assumed that the free carriers so formed will diffuse until they recombine non-radiatively. However if the excitation intensity is sufficiently large there will be an increasing probability that an electron will recombine radiatively with a free hole, thus enhancing the luminescence intensity. By assuming a simple non-radiative model of capture at defects, an exression for the luminescence efficiency is obtained

$$y_L = y_0(1+\gamma G/\beta N_S^2), \tag{29}$$

where y_0 is the efficiency determined by the ionization of pair, and γ and β are capture rates (Street 1981). This expression fits the data over a limited intensity

Fig. 21

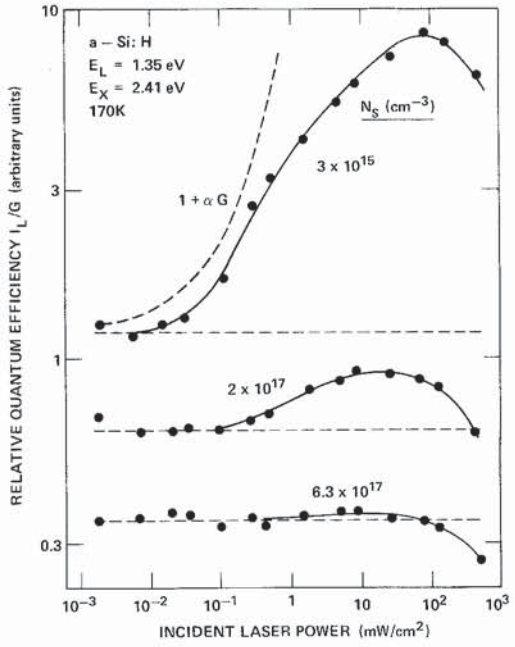

Intensity dependence of the luminescence at 170 K showing the enhancement of the quantum efficiency in samples of differing spin density (Street 1981 a).

Fig. 22

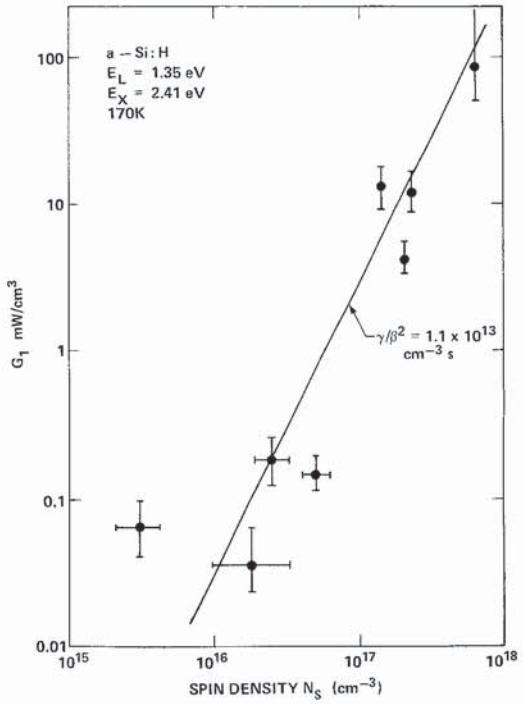

Plot showing the fit of the luminescence enhancement to eqn. (29). G_1 is the excitation intensity at which there is unity enhancement. The solid line is the dependence on N_s^{-2} expected from eqn. (29) (Street 1981 a).

range but the data does not have as strong a G-dependence as predicted. However, the dependence is N_s^{-2} is observed as shown by fig. 22. This latter result is a clear indication that dangling bonds in excess of $\sim 10^{16}\,\mathrm{cm}^{-3}$ are the primary non-radiative centres at elevated temperatures, as they were found to be at low temperatures.

A point worth emphasizing is the very low excitation intensity required to observe the effects described in this section. At low temperatures, 1 mW of unfocused laser power at 5145 Å, for example, is already in the bimolecular region (see fig. 19). From fig. 21, at the lowest defect density, the linear region is barely obtained even by going down to an excitation power of 10^{-3} mW. These results imply that most experimental results reported involve high excitation effects, the exception being pulsed experiments in which these effects are usually easier to avoid. It seems highly likely that the intensity dependent processes are at least partially responsible for the great variability in the temperature dependence data. It should be emphasized that it is virtually impossible to interpret the temperature dependence data unless the measurements are in the low intensity linear region. The condition for which this is obtained depends on the defect density, but as shown in fig. 12, that too can change the temperature dependence.

2.3.5. *Excitation energy effects and surface recombination*

When the excitation energy E_x is varied, the absorption depth, the excitation density, and the kinetic energy given to the carriers, are each varied. It is important to separate these different effects to interpret correctly the changes in the luminescence properties. The first observation of an excitation energy effect was by Rehm and Fischer (1979) who found that as E_x increased, the time constant of the initial luminescence decay decreased. They inferred that a competing non-radiative process was operating, and attributed this to surface recombination on account of the decreasing absorption depth. Recently however, Shah *et al.* (1980 b) have observed the opposite result, that the initial decay in fact has a longer decay time at high E_x. These measurements shown in fig. 23 were performed by keeping the excitation density constant. Shah *et al.* (1980 b) suggest that the opposite results of Rehm and Fischer are in fact due to an increasing excitation density as the absorption depth is decreased by raising E_x. They show that the initial decay time does in fact decrease as the excitation density is increased in agreement with the long time decay data presented in the preceding section. Figure 20 also shows that the excitation-intensity dependence of the luminescence becomes sublinear when the pair density exceeds about 10^{18} cm $^{-3}$, indicating the onset of a non-radiative process which would explain the faster decay. In addition, the data of fig. 20 agrees with the evidence for non-radiative Auger recombination whose onset is at a similar pair density, as described in §2.3.4. However, it should be noted that Rehm and Fischer (1979) investigated the intensity dependence of the initial decay but found no change. It is not clear why their data is different from that of Shah *et al.* (1980 b).

It seems likely therefore that the true effect of increasing E_x is to increase, rather than decrease the decay time. The Onsager (1938) model can provide an interpretation of the longer decay times at high E_x, because as E_x increases, the carriers are

Fig. 23

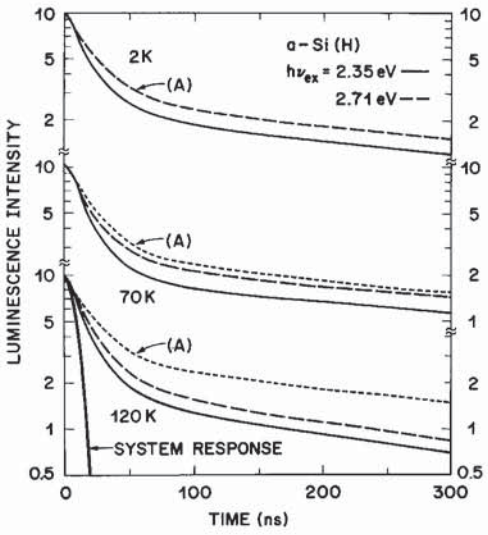

Initial decay of luminescence at two excitation energies, but maintaining a constant excitation density. The curve marked A in the upper plot is repeated in the lower plots for convenience of comparison (Shah *et al.* 1980 b).

excited with a larger excess kinetic energy, and will tend to diffuse further apart. Within the radiative tunnelling model the increased separation of the electron and hole will result in an increase in the average decay time, and presumably therefore slower initial decay of the luminescence.

Although it seems that the changes in the initial decay may not be attributed to surface recombination, there is other evidence for this mechanism. Rehm *et al.* (1980) find that the initial decay depends on the sample thickness as shown in fig. 24. Since the excitation density does not depend on thickness, these results are good evidence for surface recombination. The mechanisms considered to give this effect are either localized states at the surface or the space charge field due to band bending near the surface. Rehm *et al.* (1980) conclude that the internal electric field provides the most likely mechanism. They cite evidence that defects do not change the luminescence decay time, but that internal fields do. This is contrary to other reports which find exactly the reverse (Tsang and Street 1978, 1979). It seems to us rather unlikely that band bending can explain this data, because optical excitation tends to flatten the bands and remove the internal field (Dunstan 1981 and see below). On the other hand, there are experiments which indicate that defect or impurity states do occur at the a-Si : H surface, or oxide interface (Fritzsche 1981, Knights *et al.* 1977, Street and Knights 1981). We believe that these are the most likely source of the surface recombination effect.

The experiments described above use the initial luminescence decay as a probe of various effects. It is worth commenting that the decay up to about 10^{-7} s constitutes only a very small fraction of luminescence events, perhaps as low as 10^{-4}, and may be dominated by the non-radiative processes. One must be cautious in relating these fast events to the bulk of the recombination which has a time constant of 10^{-3} s.

The influence of surface band bending on the luminescence has been studied by superimposing a white light bias on a low intensity modulated monochromatic excitation source (Dunstan 1981). Figure 25 shows data from which it is concluded that the bias light increases the luminescence intensity when the modulated source has an absorption depth of 0·1 μm, but there is no change for weakly absorbed light.

Fig. 24

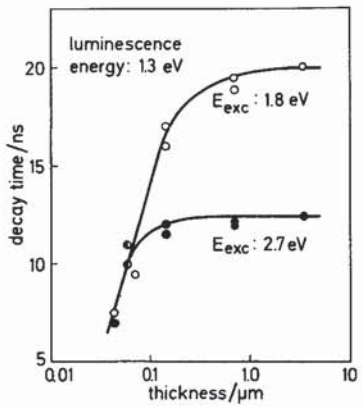

Dependence of the initial decay on sample thickness for two different excitation energies (Rehm *et al.* 1981).

Fig. 25

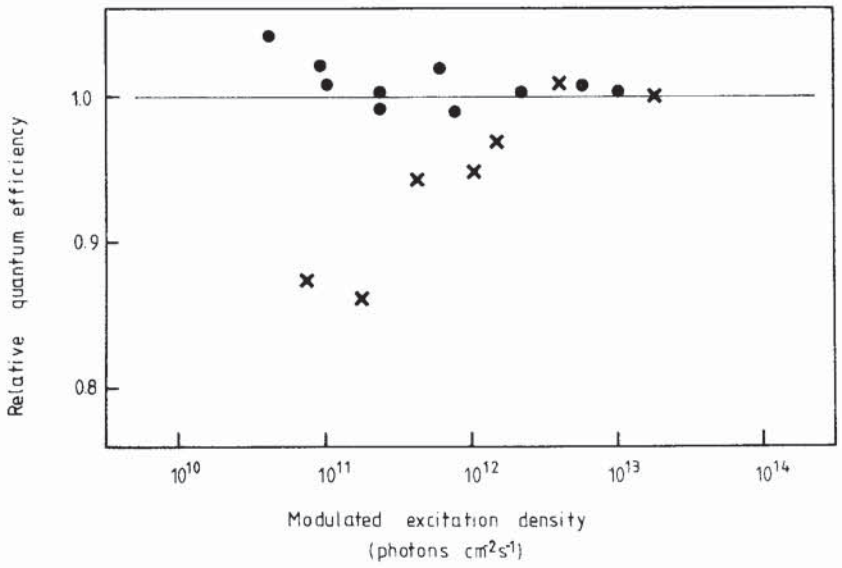

The relative quantum efficiency at different excitation densities of a sample of a-Si:H annealed to 150°C. The circles are for red excitation and the crosses for blue, on the substrate side of the sample (Dunstan 1981).

The increase of luminescence is largest at the lowest excitation intensities. The interpretation of these data is that electric fields due to surface band bending quench the near-surface luminescence. The white light bias removes the band bending and so increases the luminescence efficiency. Dunstan (1981) shows that the effect depends on the history of the sample and is absent on surfaces at which no band bending occurs. Note that an excitation flux of only 10^{12} photons $cm^{-2} s^{-1}$ will remove the band bending. This intensity corresponds to $\sim 10^{14}$ electron–hole pairs cm^{-3} (assuming $\tau \simeq 10^{-3}$ s and an absorption depth of 1000 Å). Rehm *et al.* (1980) used much higher excitation densities in the experiments described above, and so should be well into the flat band condition.

The last effect to be discussed in this section is the dependence of the luminescence energy on excitation energy (Chen *et al.* 1981, Shah 1981). When E_x is greater than about 1·8 eV, the luminescence peak has a constant energy, whereas for $E_x < 1{\cdot}8$ eV, there is a shift to low energy. The size of the shift is approximately $(E_x - 1{\cdot}8)/2$ eV (Shah 1981). This effect is explained by assuming a thermalization gap of about 1·8 eV. Excitation at higher energy always results in electron–hole pairs that thermalize down to the same average energy levels. On the other hand excitation below 1·8 eV selects electron or hole states deeper in the band tail, and so the recombination is also at lower energy. The analysis of this effect is complicated by the fact that the excitation is a convolution of both band tail densities of states. Nevertheless, based on this model one would expect the luminescence energy to be close to the thermalization gap of 1·8 eV. The discrepancy between this energy and the observed peak at 1·4 eV is perhaps further evidence for a Stokes shift.

2.3.6. *Summary of the recombination process*

The recombination model described above involves electrons and holes in localized states. There is a moderate Stokes shift indicative of a polaron-type distortion and a highly localized carrier. On the other hand the effective Bohr radius for radiative or non-radiative tunnelling is 10–12 Å, characteristic of a rather weakly localized state. The suggested resolution of this apparent contradiction is that one partner of the electron–hole pair is strongly localized, and the other weakly localized (Tsang and Street 1978). The identity of each is not easily obtained from luminescence measurements because the transition involves both particles. However, there is strong evidence from other sources that the electron does not have a large electron–phonon coupling. The best evidence is the drift mobility for which room temperature values of $1\,cm^2/V\,s$ are observed (Tiedje *et al.* 1980). This magnitude does not seem compatible with a large distortion energy. Our model is therefore that holes carry the majority of the distortion energy, estimated to be about 0·2 eV (Street 1978).

The most common model for the recombination assumes that the transition is between band tail states. There is a great deal of evidence to support this view.

(1) The zero-phonon energy of the transition is about 1·6–1·7 eV at 10 K. Given an estimated mobility gap of 2 eV, these values imply that the combined electron and hole binding energy is roughly 0·3–0·4 eV, which is roughly the expected magnitude for band tail states.
(2) The most efficient luminescence occurs in samples of the lowest defect density and with 'optimum' electronic properties. This implies that the states involved in luminescence are intrinsic in the sense that band tail states are a property of the ideal amorphous network, rather than being defect or impurity states.
(3) The luminescence excitation spectrum follows the fundamental absorption edge without any evidence of an extrinsic process.
(4) The relatively low temperature at which thermal quenching occurs implies that at least one carrier is within 0·2 eV of the mobility edge.
(5) The density of states involved in the luminescence is at least $10^{18}\,cm^{-3}$, and probably much higher (see fig. 20). If one accepts the evidence of field effect data, then in low defect density material, a density of states this large is only found in the band tails, or possibly in the E_γ band above the valence band edge (Madan *et al.* 1976).

In fact, Tsang and Street (1979) have suggested that the E_γ band arises from self-trapped holes split off from the valence band tail which participate in the luminescence. It is argued that the electron–phonon interaction need not apply equally to every valence band state as would be the case for conventional small polarons in a crystal. Instead, by its very nature, the amorphous network allows for a distribution in the local potential due to bond length and bond angle distortions, etc. The electron–phonon interaction may occur preferentially at a small fraction of states at which the bonding distortions are greatest, and which tend to localize holes most strongly. The effect would be that part of the band tail, presumably corresponding to states above a certain energy, would tend to split off from the rest of the band tail because of the distortion. Tsang and Street (1979) suggest that these split off states are the origin of the E_γ band. This is a speculation for which there is little evidence beyond the observation of the Stokes shift. This model predicts that

Fig. 26

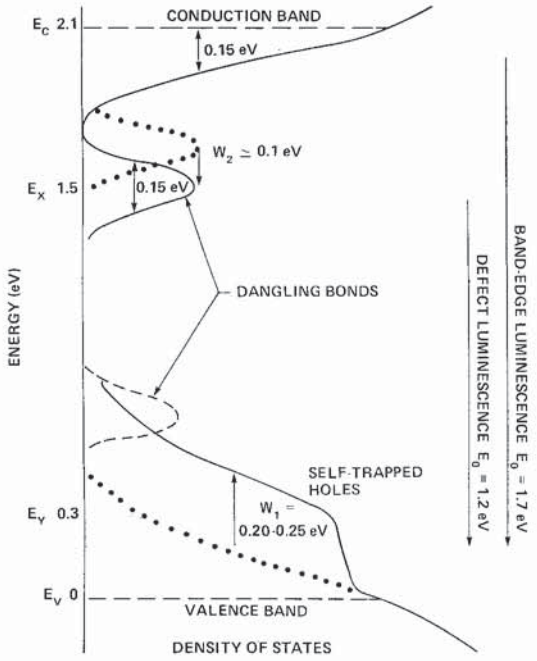

Schematic density of states diagram based on the luminescence data. W_1 and W_2 are estimated distortion energies (Street 1980 b).

holes would have a trap-limited transport with an activation energy which is the sum of the distortion energy and the additional initial localization energy. The observed hole activation energy of 0·35 eV is therefore consistent with the model. Figure 26 shows a schematic density of states diagram based on the model discussed above.

The luminescence experiments on a-Si : H demonstrate a variety of recombination mechanisms for the band edge transition which are summarized below.

(1) Geminate radiative recombination. This is the dominant recombination mechanism in low defect density material at low temperature and low excitation intensity. It is a monomolecular process involving isolated electron–hole pairs.

(2) Non-geminate radiative recombination. This mechanism occurs at high excitation intensities when electron–hole pairs are not isolated, and is a bimolecular process.

(3) Non-radiative tunnelling to defects. When the dangling bond density exceeds about $10^{17}\,\mathrm{cm}^{-3}$, non-radiative tunnelling becomes the dominant recombination mechanism at low temperatures. The subsequent recombination of the trapped electron is discussed in §2·5.

(4) Thermal ionization of pairs. At elevated temperatures electron–hole pairs separate by a thermally activated diffusion process. If the excitation intensity is sufficiently low the free carriers are captured at defect states. At high excitation intensities the carriers can recombine radiatively in a non-geminate process.

(5) Non-radiative Auger recombination. When the excitation intensity is sufficiently high for non-geminate recombination, there is also an Auger process involving overlapping electron–hole pairs.
(6) Surface recombination. Excitation of electron–hole pairs close to a surface results in an enhanced non-radiative recombination.

We consider that the experimental evidence for each of these mechanisms is sufficiently strong that they form a fairly reliable basis for understanding other recombination properties that are described in the remainder of this review. Some of the mechanisms are still the subject of debate, and in one case described in §5·2, a new recombination mechanism has been proposed from transport data, which impacts on the luminescence models. Therefore there remains a need for new experiments to test the validity of the models discussed here.

2.4. *Other luminescence properties*

2.4.1. *Time-resolved luminescence spectra*

The luminescence decay data described in §2.3.1 provide information about the spatial distribution of the electron–hole pairs, but does not give information about the corresponding energy distribution. Much of this distribution is obscured by the line broadening of the luminescence spectrum due to the phonon interactions. The large temperature dependence of the luminescence peak energy is one experiment in which effects of the energy distribution can be observed (see §2.2.2). Measurements of the time-resolved luminescence spectrum provide further information. The experiments are performed using pulsed excitation and gating the luminescence at a fixed delay time. Examples of the time resolved spectra are shown in fig. 27. The line

Fig. 27

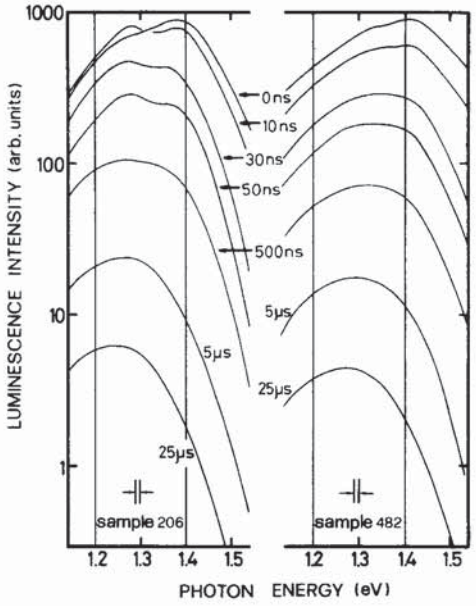

Time-resolved luminescence spectra of two samples at 77 K. Note that the change of intensity corresponds to the true time decay (Kurita *et al.* 1979).

width is almost the same as for the C.W. spectrum as is expected if phonon broadening is the dominant contribution to the width. Kurita *et al.* (1979) (fig. 27) report that at the shortest times there are two luminescence peaks separated by about 0·1 eV. After about 100 ns the high energy component becomes unresolvable. This structure has not been observed by others (Tsang and Street 1979, Street 1980 a).

Figure 28 shows that the luminescence peak shifts by about 0·15 eV over a broad time range (Tsang and Street 1979). An interesting feature is that there are apparently three time zones. Up to 10^{-6} s there is a steady decrease of the peak energy; from 10^{-6} to 10^{-4} s the peak energy is practically constant; above 10^{-4} s the energy again decreases. This separation into three zones is clarified by similar data on Si–O alloys also shown in fig. 28 (Street and Knights 1981). In these alloys the time-resolved peak shifts are larger and non-monotonic. Between 10^{-6} and 10^{-4} s the peak energy increases.

Fig. 28

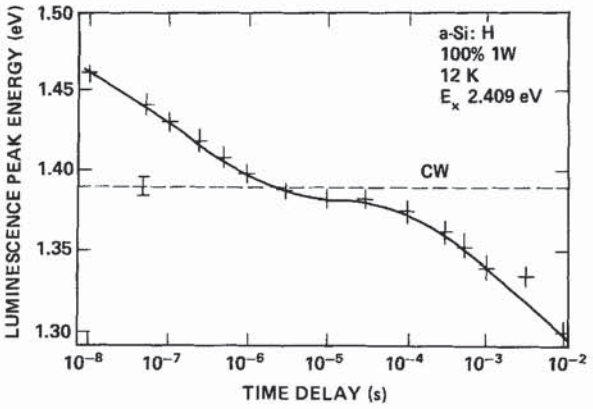

(*a*)

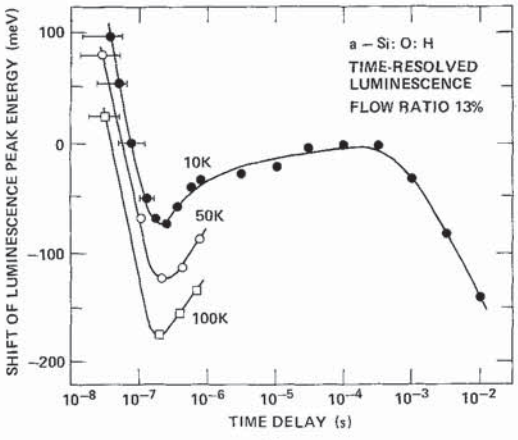

(*b*)

Time-resolved shift of the luminescence peak in a-Si : H and a-Si : O : H (Tsang and Street 1979. Street and Knights 1981).

The interpretation put forward for the time dependence is based on the recombination mechanisms described in § 2.3. Three different effects contributing to the time-resolved spectra have been discussed (Tsang and Street 1979, Street 1980 a). First there is a thermalization process, by which carriers excited high into the band will lose energy. It is expected that thermalization down to the mobility edge will be very fast, occurring in about 10^{-12} s. However, within the localized states, thermalization should be by tunnelling and the rate of these transitions will decrease rapidly as the density of available states at lower energy decreases. It is therefore proposed that the shift of the time-resolved spectra at times less than 10^{-6} s is due to the final stages of thermalization within the localized states. In these experiments the observed shift in this time range is less than 0·1 eV compared to an initial excess energy of 1 eV, so certainly most of the thermalization occurs at times too short to be resolved in these experiments.

The second mechanism is the Coulomb interaction between the electron–hole pair. Within the radiative tunnelling model, the decay time of a specific pair is determined by the electron separation R,

$$\tau = \tau_0 \exp(2R/R_0). \tag{30}$$

The Coulomb interaction also depends on the pair separation, and is therefore correlated with the decay time. Since the interaction is attractive, the luminescence energy is expected to increase with time, in the time-resolved spectra. Such behaviour is not observed in a-Si : H, but is in some Si : O alloys (see fig. 28). These alloys have a much lower dielectric constant, and therefore a larger Coulomb term, than a-Si : H. It is therefore argued that the expected increase in luminescence energy in a-Si : H is obscured by the other mechanisms that tend to shift the peak to low energy (Street 1980 a).

The third mechanism for the shift of the time-resolved spectrum originates from the energy distribution of the localized band tail states. It is expected that the Bohr radius, R_0 in eqn. (30), decreases with increasing binding energy of the electron (see, for example, Mott and Davis 1979). States with the largest binding energy therefore have the longest decay times, and a consequent shift of the luminescence to low energy at long times is expected. The time dependence of the shift can be calculated from the form of the luminescence decay data, and there is reasonable agreement between the calculation and the data for delay times greater than 10^{-4} s.

Although these three mechanisms readily account for the available data, an alternative explanation of the shift of the time-resolved spectrum below 10^{-6} s is possible. According to eqn. (30), time constants in this range correspond to electron–hole pair separations of less than about 25 Å. To achieve such small separations, with reasonable probability, the density of states must be 10^{19} cm^{-3} or larger. Thus, as a consequence of the decreasing density of states into the forbidden gap, the fast luminescence may correspond to electrons and holes that tend to lie closer to the mobility edges than the average. This possibility deserves further investigation.

The shift of the time-resolved spectrum involves a complex interplay of at least three different mechanisms and involves both the spatial and energy distribution of the electron–hole pairs. For this reason the experiments give qualitative information but it is not yet possible to obtain the detailed energy distribution. However, the total shift of the luminescence, $\sim$0·15 eV, is in line with various estimates of the width of the band tails.

2.4.2. *Electric field dependence and electroluminescence*

Engemann and Fischer (1976) and Pankove and Carlson (1976) observed that an applied electric field of 10^5 V/cm or greater will quench the luminescence intensity. The effect is found to depend on the excitation energy in a rather unsystematic manner, as shown in fig. 29, and the quenching can be as large as 90% (Nashashibi *et al.* 1977 b). The natural interpretation of the effect is the ionization of electron–hole pairs by the field and a good fit to a Poole–Frenkel expression is found (Paesler and Paul 1980). Within the model of electron–hole pairs occupying band tail states, the mechanism is presumably field ionization of the localized electron. Assuming an electron binding energy of 0·1 eV and an electric field of 10^5 V/cm, then the electron would have to tunnel 100 Å to reach the mobility edge. This distance is reasonable for a Bohr radius of about 10 Å, and indeed is similar to the distance for a non-radiative transition according to the model described in § 2.3.2. This explanation of the field quenching predicts that the shallow electrons are most easily ionized, and so the electric field should shift the luminescence peak to low energy. This effect has been observed by Street *et al.* (1979 b), but apparently not by Nashashibi *et al.* (1977 b).

Pankove and Carlson (1976) first reported electroluminescence from a-Si : H p–i–n junctions and Schottky barriers, using an electric field of about 3×10^5 V/cm. They found that the spectrum was essentially the same as that observed in photoluminescence. Other groups have also reported electroluminescence, and in one case the spectrum is observed to be shifted to low energy by about 0·1 eV (Street *et al.* 1979 b). It is evident that electroluminescence can only be observed if one or other carrier crosses the sample, and it is generally assumed that this must be the electron although there is no direct evidence. It is interesting to note that the field strengths used in both the electroluminescence, and the electric field quenching experiments are very similar. It is therefore possible that some part of the field quenching effect is due to the macroscopic movement of charge across the sample, rather than simply the local ionization of an electron–hole pair.

2.4.3. *Pressure dependence*

The application of hydrostatic pressure of up to 50 kbar, using a diamond anvil, shifts the luminescence peak to low energy with a pressure coefficient of

Fig. 29

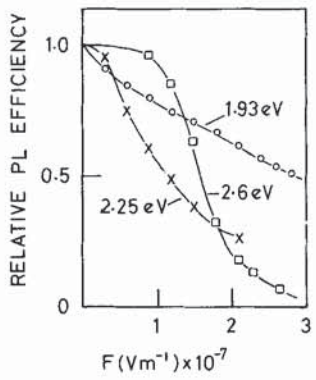

Electric field dependence of the luminescence intensity at 77 K for various excitation energies (Nashashibi *et al.* 1977 b).

Fig. 30

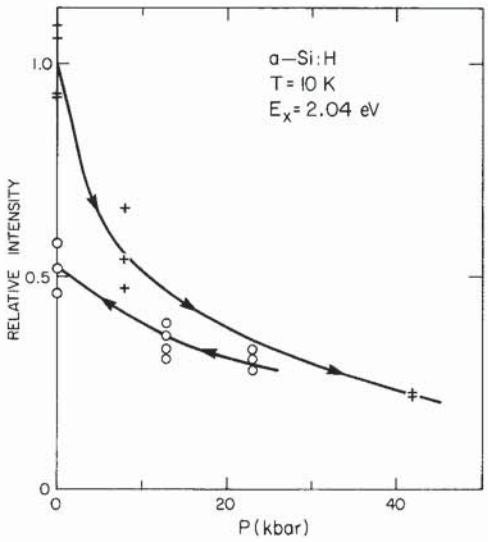

Pressure dependence of the luminescence intensity showing both reversible and irreversible effects (Weinstein 1981).

$-2{\cdot}0 \pm 0{\cdot}5$ meV/kbar (Weinstein 1981). Pressure also quenches the luminescence intensity by a factor of 5 at 50 kbar. After the pressure is released, the intensity returns only to about 50% of its original value, indicating an irreversible structural change. The data are shown in fig. 30. The quenching is interpreted as due to the formation of excess dangling bonds with density about 10^{17} cm^{-3}. The mechanism is thought to be the collapse of internal voids resulting in the rupturing of bonds. The decay data at low pressure (up to 25 kbar) support this interpretation because the decay times are observed to decrease. However, above 25 kbar the decay times increase, and the result is hard to account for. It would be very informative to have an independent measure of the dangling bond density at high pressure, for example by E.S.R., but this is a difficult experiment. It would also be interesting to know whether the irreversible changes observed with pressure are in any way related to the increase in dangling bond density caused by prolonged illumination, as described in § 4.3.

The pressure shift of the luminescence is similar to that observed for the absorption edge. This result supports the model that the luminescence originates from a band-to-band transition. The additional supposition of a Stokes shift is also tested by the pressure dependence data and reasonable compatibility within rather wide limits, is obtained.

2.4.4. *Spin dependent luminescence*

Following experiments by Lepine (1972) on crystalline silicon, it was discovered that the photoconductivity of amorphous silicon was spin dependent (Solomon *et al.* 1977). By this is meant that when electron spins are in resonance by the application of a suitable magnetic field and microwave power, the magnitude of the photoconductivity changes. Following this observation a similar effect was observed in the

luminescence of a-Si : H (Biegelsen *et al.* 1978, Morigaki *et al.* 1978). The measurement of spin dependent luminescence, S.D.P.L., (also called optically detected magnetic resonance O.D.M.R.) is generally performed in an E.S.R. cavity. The microwave power is chopped at a chosen frequency and the coherent change in the luminescence is measured using lock-in detection. The magnetic field is then swept through the resonance to obtain the S.D.P.L. resonance. The measurements relate to the details of the spin interactions of the recombining electron and hole, and in principle are a very sensitive test of the recombination models.

The basic experimental results were reported at about the same time by Morigaki *et al.* (1978) and Biegelsen *et al.* (1978). Either an increase or a decrease in the luminescence can be observed at the resonance, depending on the experimental conditions. These are referred to as enhancing or quenching lines respectively. Above about 40 K, only quenching lines are observed, and an example of the resonance spectrum is shown in fig. 31. The peak is close to $g=2{\cdot}005$ and has a line width and asymmetrical shape which is very similar to that observed in light induced E.S.R. (Knights *et al.* 1977). The L.E.S.R. is known to consist of two resonances, and in other experiments the two quenching lines are observed explicitly in S.D.P.L. (see fig. 31). The relative change in the luminescence intensity at resonance, $\Delta L/L$, is $\sim 10^{-3}$, and is almost independent of temperature up to at least 100 K.

Below 40 K, there is an enhancing signal in addition to the quenching lines. Figure 32 shows an example of the resonance spectrum at 2 K. The enhancing line has a width of about 200 G which is much broader than any E.S.R. resonance observed in a-Si : H. The width increases with microwave power, and the shape also changes with chopping frequency. At high frequency, >1kHz, a narrow enhancing resonance with a width 32 G is seen. Both enhancing lines are strongly temperature dependent, decreasing approximately as T^{-2}.

The data on the spectral dependence of the S.D.P.L. are a little unclear. Morigaki *et al.* (1978) report that the strength of the quenching lines is largest on the high energy side of the luminescence spectrum, and that the enhancing lines are greatest on the low energy side. Biegelsen *et al.* (1978) agree with these results for the enhancing lines, but find that the quenching lines are independent of the lumines-

Fig. 31

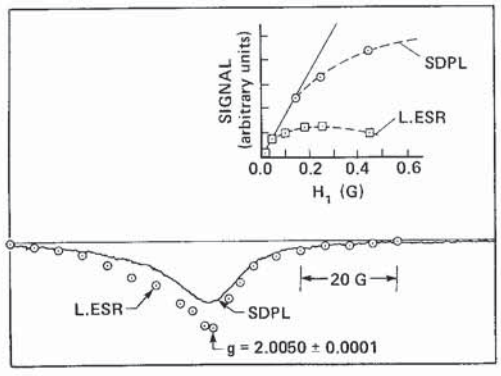

Spin dependent luminescence quenching signal compared to the light induced E.S.R. resonance at 80 K. Inset shows the microwave saturation of the two experiments (Biegelsen *et al.* 1978).